Design and Dynamic Stiffness Evaluation of Magnetorheological Elastomer Bushing using FEMM and Dynamic Testing Machine

Mohamad Ihsan Abdul Hamid, Saiful Amri Mazlan, Nur Azmah Nordin
Engineering Materials & Structures (eMast) Ikhoza,
Malaysia-Japan International Institute of Technology (MJIIT),
Universiti Teknologi Malaysia, 54100 Kuala Lumpur, MALAYSIA

Abdul Yasser Abd Fatah[*]
Department of Engineering and Technology,
Razak Faculty of Technology and Informatics,
Universiti Teknologi Malaysia,
Jalan Sultan Yahya Petra, 54100 Kuala Lumpur, MALAYSIA
[*]*yasser.kl@utm.my*

Ubaidillah, Fitrian Imaduddin
Mechanical Engineering Department, Faculty of Engineering,
Universitas Sebelas Maret,
Jl. Ir. Sutami 36A, Kentingan, Surakarta 57126, Central Java, INDONESIA

Fitrian Imaduddin
Department of Mechanical Engineering, Islamic University of Madinah,
Medina 42351, SAUDI ARABIA

Izwan Ismail
Faculty of Manufacturing and Mechatronics Engineering Technology,
Universiti Malaysia Pahang, 26600 Pekan, Pahang, MALAYSIA

ABSTRACT

This research presents a simulation study on electromagnetic behaviour of magnetic flux density distribution in a magnetorheological elastomer (MRE) bushing. The design concept of MRE bushing is based on the design of the bushing used in the conventional car, only the natural rubber is being replaced by the MRE compound. Furthermore, the electromagnetic simulations were

ISSN 1823-5514, eISSN 2550-164X
Received for review: 2022-03-02
Accepted for publication: 2022-08-19
Published: 2023-01-15

https://doi.org/10.24191/jmeche.v20i1.21077

conducted by using Finite Element Method Magnetics (FEMM) software where the main aim is for more magnetic flux density in the MRE, which indicates better performances for MRE bushing in this study. The best configuration of the MRE bushing for this study is using single coil, magnetic material for all parts except for coil bobbin, and the thickness of ring plate of 4 mm, which yield the highest magnetic flux density of 0.205 T. By using this configuration, the dynamic stiffness of this MRE bushing is ranging from 2259.13 N/mm to 2671.06 N/mm with the applied currents of 0.5 A to 2.5 A and frequencies from 1 Hz to 15 Hz. All in all, the optimized configurations improve the performance of MRE bushing remarkably.

Keywords: *Magnetorheological Elastomer (MRE); MRE Bushing; Electromagnetic; FEMM; Dynamic Stiffness*

Introduction

Magnetorheological elastomer (MRE) is a branch of smart materials that is rapidly evolving and actively studied by other researchers [1]-[4]. In particular, MRE provides an active response by the presence of magnetic field to change the rheological properties of the MRE continuously, rapidly, and reversibly. MRE is made up of matrix, magnetic particles and also additives [5]-[10]. Due to the ability of the MRE that can be changed rheologically, the stiffness and damping of MRE can be controlled by the magnetic field using an electromagnetic circuit [11].

Many researchers have incorporated MRE into diverse applications, such as isolator, engine mount, and prosthetics device [12]-[16]. Since then, these devices managed to achieve controllable stiffness and thus, acted as a vibration absorber based on their applications. Apart from that, MRE compound also being used in the development of the MRE bushing, where there are a few studies regarding that matter [17]-[20]. With the help of MRE, the MRE bushing managed to control and reduce the vibration, thus, decreasing the external loadings and transmitting the vibrations between parts.

Conventional rubber bushing had a passive behaviour that mainly used natural rubber (NR) as its compound. Consequently, conventional bushing had fixed stiffness characteristics, which can only cater to a certain rigid range of stiffness [21]. Therefore, Kumbhar et al. [17] had developed an MRE bushing and compared it with the conventional bushing for transmissibility in terms of isolation between that two devices. Furthermore, Elie et al. [19] and Ginder et al. [20] had designed another type of MRE bushing and measured the stiffness while varying the applied current. These studies showed the reaction of MRE bushing to the applied current where the higher the applied current, the higher force and stiffness obtained. Meanwhile, Blom et al. [22] conducted an engineering stiffness formula that predicts the frequency and amplitude

dependent stiffness of MRE bushing. From these calculations, it predicted and clearly displayed the possibility of controlling the stiffness of MRE bushing over a large frequency range. In addition, Kim et al. [23] did a simulation for MRE bushing based on their design for magnetic field analysis.

However, further studies are vital for the design of MRE bushing. In fact, other elements for the development of MRE bushings such as the design and simulation configurations, are not adequately investigated. Thus, in this study, an asymmetrical model of an MRE bushing was designed and simulated using Finite Element Method Magnetics (FEMM) software. From the FEMM simulation, the magnetic flux was flown through the MRE, hence, the magnetic flux density within the MRE can be determined. The performance of MRE bushing is depending on the amount of magnetic flux density flown into the MRE bushing, which translated into adjustable dynamic stiffness. Therefore, the configuration of the coil, the material selections, and geometrical dimensions in designing the MRE bushing was determined and considered to enhance the performance of the MRE bushing respectively. The best configuration based on simulation analysis is achieved and that design proceeds for the experimental testing of dynamic stiffness.

Design of MRE Bushing using FEMM

The design of MRE bushing in this study is based on the design of the bushing used in the conventional car. The main difference between the conventional bushing and the MRE bushing is the compound used, where the NR is used for conventional bushing, while the MRE bushing will be using natural rubber-based MRE (NR-MRE). The structural design of this MRE bushing is influenced by prior works which suitable for industrial and research scales [17], [19]-[20], [24]-[25]. Mainly, the structural design of the MRE bushing has been enhanced so that the ultimate aims have been achieved. In addition, an electromagnetic circuit is also added into the device for generating the magnetic field by manipulating the input current.

The next steps for designing the MRE bushing are the material selection and geometrical dimension of parts. For this design the important criteria are the overall size of the MRE bushing, the thickness of parts, the selection of the materials, and the design of coil. Notwithstanding, these design criteria can affect the outcome performance of MRE bushing. Therefore, this MRE bushing has been designed to utilize the controllable stiffness ability of MRE.

In this design, the MRE bushing is comprised of five main parts. The first part corresponds to the top and bottom ring plates. Next is the MRE, where the stiffness of the bushing can be adjusted, and vibration absorption happened. Then, the inner and outer pipes, where they sandwiched the MRE compound in the device. The fourth part is referred to as the electromagnetic coil that wound around the coil bobbin, which is made of aluminium, a non-magnetic

material. Lastly is the housing, where it covers all the aforementioned parts. Figure 1 shows the axisymmetric conceptual design of the MRE bushing used for this study. Meanwhile, Table 1 shows the structure parameter of the MRE bushing.

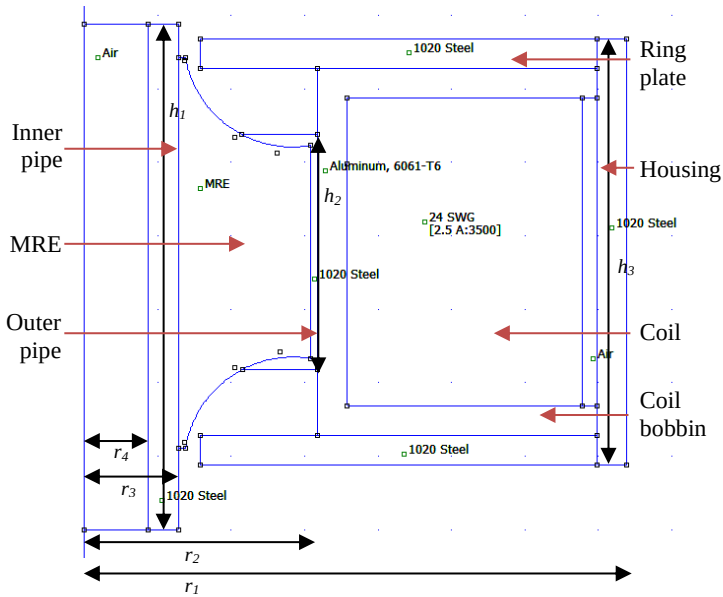

Figure 1: Axisymmetric conceptual design of the MRE bushing

Table 1: Structure parameter of the MRE bushing

Item	Parameter	Value (mm)
r_1	Radius of the structure	50
r_2	Radius of the bushing	25
r_3	Inner radius of the MRE	7.5
r_4	Inner radius of the inner pipe	5
h_1	Height of the inner pipe	69
h_2	Height of the outer pipe	32
h_3	Height of the cylindrical housing	50

For the coil, the wire is calculated to be 3500 turns based on the size allocated for the coil and the wire type of SWG 24. From the work of Fatah et al. [26], number of turns of coil configuration are based on the diameter of the wire and the dimension of the coil bobbin. The electromagnetic coil is wound around a cylindrical coil bobbin and placed internally within the housing in order to generate magnetic field inside the MRE bushing. By placing it

internally, the magnetic field strength can be distributed directly into the MRE effective area of the bushing. The effective area is referring to the MRE compound as it produces the stiffness of the device since it has the viscoelastic behaviour. The investigation on the effective area can be seen in other prior works of MRE devices as well [13], [16], [27]-[28].

Besides the coil, each part is also important to guide the magnetic flux density across the MRE bushing. The arrangement of parts in the design also plays an important role as well. By placing the combination of metal as a magnetic material and aluminium as a non-magnetic material, the flux can be guided to allow or avoid areas in the MRE bushing. Other than that, the material selection is also important in doing the same task of guiding the magnetic flux. Besides the use of metal and aluminium, the NR-MRE is another material used in the MRE bushing. It is used for adjusting the dynamic stiffness of the device based on the presence of magnetic flux density. Thus, the attributes of NR-MRE are being input into FEMM based on B-H curve data obtained from the vibrating sample magnetometer (VSM) test [13]. The list of all the parts used is shown in Table 2.

Table 2: List of parts and material for MRE bushing

Part Name	Type of Material	Material	Type
Ring plate	Magnetic	Low carbon steel	AISI 1020
Elastomer	Magnetic	MRE	NR-MRE
Inner pipe	Magnetic	Low carbon steel	AISI 1020
Outer pipe	Magnetic	Low carbon steel	AISI 1020
Coil bobbin	Non-magnetic	Aluminum	6061-T6
Electromagnetic Coil	Non-magnetic	Copper wire	SWG 24
Housing	Magnetic	Low carbon steel	AISI 1020

For MRE bushing, one of the most significant factors to consider is electromagnetic performance. It is referring to the investigation on the electromagnetic circuit design. In this research, simulation of the electromagnetic circuit design was done using FEMM. It is used to simulate and analyze the electromagnetic circuit design for the MRE bushing. In addition, FEMM is practical for analysing magnetic behaviour and magnetic field strength inside the effective region of the MRE bushing. Thus, an axisymmetric two-dimensional (2D) cross-section of the MRE bushing is drawn in the FEMM. After that, the type of materials is being assigned for each part of MRE bushing.

Moreover, the coefficients in a boundary condition for an asymptotic boundary condition can be represented by Equation (1) as follows:

$$\frac{1}{\mu_r \mu_o} \frac{\partial A}{\partial n} + c_o A + c_1 = 0 \tag{1}$$

where A is the magnetic vector potential, μ_r is the relative magnetic permeability of the region adjacent to the boundary, μ_o is the permeability of free space, and n represents the direction normal to the boundary. Coefficients of c_0 and c_1 can be represented by Equation (2) and Equation (3) as follows:

$$c_o = \frac{1}{\mu_r \mu_o R} \tag{2}$$

$$c_1 = 0 \tag{3}$$

where R is the outer radius of a sphere problem domain.

After the designing stage, applying the boundary conditions, and inputting all of the material properties, the 2D MRE bushing model is then being analysed in the FEMM. 2.5 A current is being applied to generate the magnetic field across the effective area of MRE bushing. 2.5 A is the maximum applied current in this study for simulation and experimental. The data from this simulation is then collected and analysed to investigate the performances of the bushing during the presence of magnetic field, therefore the distribution of the magnetic flux in the MRE bushing can be observed. The distribution of magnetic flux of the MRE bushing in the FEMM is shown in Figure 2. FEMM helps to adjust different configurations applied to the MRE bushing such as the electromagnetic coil configuration, the materials configuration of parts, and the geometrical configuration of parts.

For the coil configuration, there are three configurations considered for the design of coil in the electromagnetic circuit: single, double and triple coils. As mentioned by Fatah et al. [26], the configuration of coil can be divided into two, which are single and multiple coils. The differences between single and multiple coils used in MRE bushing are significant, as it involves different ways to arrange the magnetic flux path in the bushing. Besides, for the materials selections, they are selected from the use of either magnetic (AISI 1020), or non-magnetic materials (Al 6061-T6), or a combination of both. Lastly, the geometrical configuration is based on the effects of the thickness of ring plates with configuration from 1 mm to 4 mm with the increment of 1 mm. All in all, this configuration analysis of MRE bushing lead to the optimized performance remarkably.

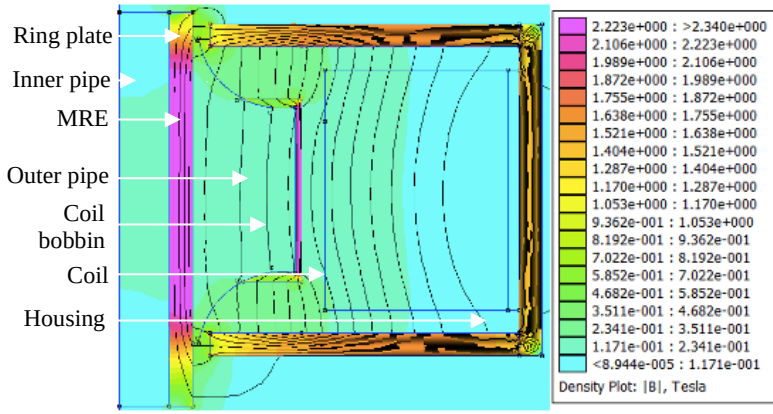

Figure 2: Simulated of magnetic flux density in MRE bushing

Experimental Setup

The dynamic compression test was performed to observe the dynamic stiffness from various frequencies by using a servopulser test machine (Shimadzu) equipped with a 20-kN load cell. The test machine for this experimental setup is shown in Figures 3. By using this machine, the MRE bushing can experimentally tested using frequency sweep method to observe the stiffness characteristic of MRE bushing, from increasing frequencies under different applied current. In addition, this experiment is a non-destructive test conducted to determine the MRE bushing behavior towards the dynamic performance in terms of stiffness characteristic on varied applied frequencies.

The test is performed under the compression behavior with the presence of magnetic field by supplying input currents from 0.5 to 2.5 A with an interval of 0.5 A, and the amplitude was fixed at 1.0 mm. When the current is applied, the frequency sweep begins from 1 Hz (low frequency) to 15 Hz (high frequency). Then, the same procedure was applied to the same sample but with different current input.

Before the experiment is done, a jig is mounted to an exciter and a load cell accordingly to hold the MRE bushing. This jig is made of aluminum so that it will not be affected by the magnetic field to prevent the magnetic field distortion. A shaft is inserted into the inner pipe of MRE bushing to join the bottom brackets that are mounted to the testing machine. The 20-kN load cell is installed on top of the jig to measure the load applied to the MRE bushing. The wire coil from MRE bushing is connected to the voltage regulator to provide the input current. The voltage regulator was supplied with 5760 watt (240 V x 24 A) to generate magnetic field to the MRE bushing throughout the

experiment. Table 3 shows a summary of the variable arrangement of the experimental test.

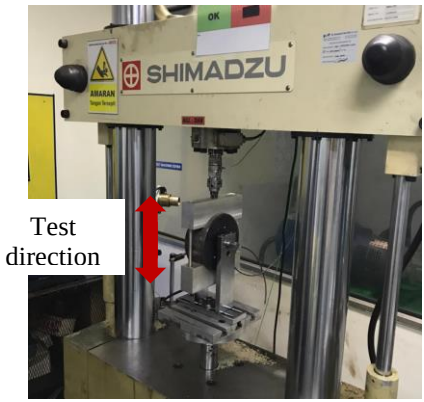

Figure 3: Experimental setup that show the testing machine for assessing the stiffness of the MRE bushing

Table 3: Summary of the variable arrangement of experimental test

Frequency sweep (Hz)	Excitation Amplitude (mm)	Input Current (A)
1 - 15	± 1.0	0.5 – 2.5

Results and Discussions

The results and discussion shown are from the FEMM simulation and experiment done to get the optimum performance of the bushing from the parameters tested. These include coil configurations, materials configuration of parts, geometrical configuration, and the dynamic stiffness from the experimental testing. For the simulation, the results are based on the average value of magnetic flux density at the effective area in the MRE bushing (Figure 4). For the current input, it is set at a constant of 2.5 A for simulation, however it is set ranging from 0.5 A to 2.5 A for experimental testing.

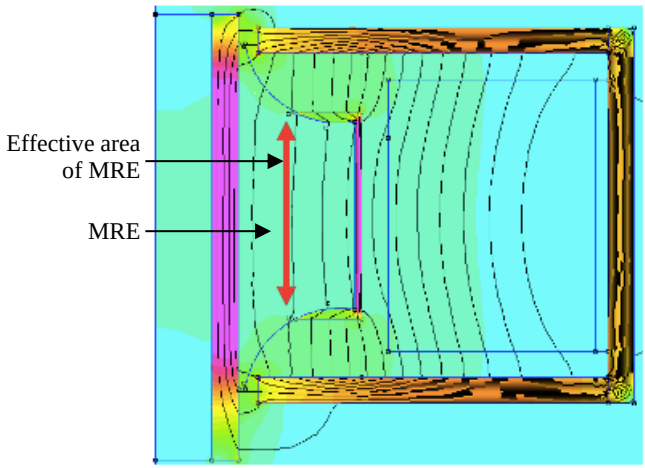

Figure 4: The effective area of MRE bushing

MRE bushing performance based on coil configurations

The coil configurations can lead to the maximum magnetic flux density in the MRE bushing. As previously mentioned, there are three configurations considered for the design of coil in the electromagnetic circuit: single, double and triple coils (Figure 5). The average values of magnetic flux density were taken at the same position in the bushing, which is the effective area in the MRE.

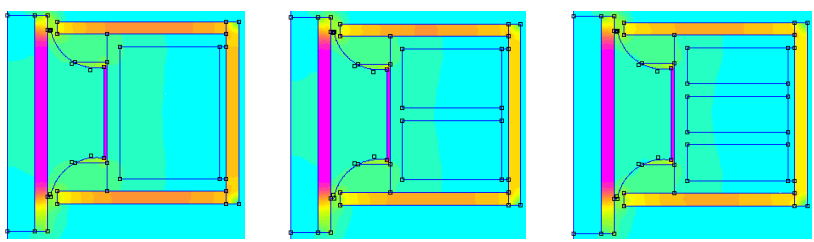

Figure 5: Design and arrangement of coil configurations for MRE bushing; (a) single coil (b) double coils, and (c) triple coils

For the single coil, the MRE bushing is designed with 3500 turns. Meanwhile, the double coil consisted of 1500 turns on each coil and triple coil has 900 turns on each coil. Based on the simulation analysis, the bushing with a single coil produces the highest value of the magnetic flux density at 0.21 T,

followed by double coil (0.17 T), and triple coil at 0.15 T. Figure 6 shows the magnetic flux density for these three configurations.

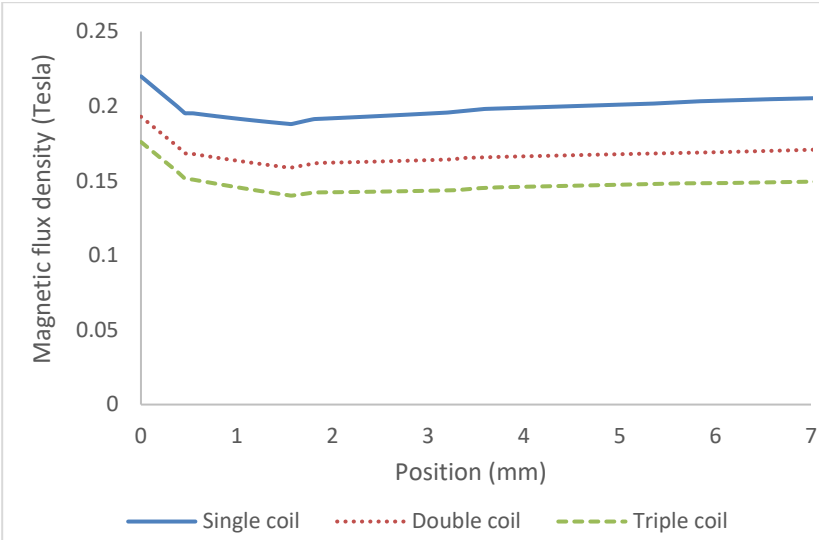

Figure 6: Magnetic flux density for different configurations of coil

From the graph, the single coil produced the highest magnetic field strength in the MRE effective area, and the double and triple coil yield lower magnetic flux density because the flux encircled the coil bobbin with uneven magnetic field strength and had the highest magnetic flux leakage compared to the single coil. In addition, the total number of coils turns needed to be divided by two or three coils, and thus, it was affecting the amount of magnetic flux flowing through the center of the bushing. Thus, the single is selected for the design of MRE bushing.

Material configurations of parts

The material configurations are based on the influence of the material on the distribution of the magnetic flux in the effective area of the MRE bushing. For this analysis, the parts of MRE bushing consisted of the use of magnetic (AISI 1020) or non-magnetic materials (Al 6061-T6), or both. Then, the selection of materials is done to obtain the highest magnetic flux density at the effective area of the MRE bushing respectively. Thus, the parts for MRE bushing such as inner and outer pipes, housing, and ring plates have been simulated by alternately changed between magnetic and non-magnetic materials except for coil bobbin which remains as non-magnetic material (Al 6061-T6). Based on the FEMM simulation done, each of the parts is made from the magnetic

material that has high magnetic permeability and magnetic saturation. Table 4 shows different combinations of material selections for the parts of MRE bushing.

Table 4: The material selections of MRE bushing parts

Design	Inner Pipe	Outer Pipe	MRE	Coil bobbin	Coil	Ring Plate	Housing
A	Magnetic	Magnetic	Magnetic	Non-magnetic	Non-magnetic	Magnetic	Magnetic
B	Non-magnetic	Magnetic	Magnetic	Non-magnetic	Non-magnetic	Non-magnetic	Non-magnetic
C	Magnetic	Non-magnetic	Magnetic	Non-magnetic	Non-magnetic	Magnetic	Non-magnetic
D	Non-magnetic	Non-magnetic	Magnetic	Non-magnetic	Non-magnetic	Non-magnetic	Magnetic
E	Non-magnetic	Non-Magnetic	Magnetic	Non-magnetic	Non-magnetic	Non-magnetic	Non-magnetic
F	Magnetic	Magnetic	Magnetic	Non-magnetic	Non-magnetic	Non-magnetic	Non-magnetic
G	Magnetic	Non-Magnetic	Magnetic	Non-magnetic	Non-magnetic	Non-magnetic	Non-magnetic

Figure 7 shows the magnetic flux density at the effective area of MRE bushing for the different configurations of MRE bushing materials. The order of the design from the highest to the lowest value of average magnetic flux density are as follows: A (0.205 T), C (0.177 T), D (0.14 T), E (0.136 T), B (0.087 T), G (0.085 T), and F (0.048 T). Based on this order, design A which has the highest value of magnetic flux density is chosen for the design of MRE bushing. The combinations of magnetic and non-magnetic material for design A are optimum for this MRE bushing, where the inner and outer pipe, ring plate, and housing are from a magnetic material, while the coil bobbin is from non-magnetic material. This is because, the use of magnetic materials for inner and outer pipe, ring plate, and housing shows higher flux density in the effective region than any other combination. Consequently, higher magnetic flux can enhance the performance of MRE bushing respectively.

Geometrical configuration of part of MRE bushing

The geometrical configuration is based on the effects of the thickness of ring plates to the distribution of the magnetic flux in the effective area of the MRE bushing, where they guide the magnetic flux through the MRE and prevent it leaked from the MRE bushing. For this reason, the thickness of ring plates is configured from 1 mm to 4 mm with the increment of 1 mm as shown in Figure 8. In this finding, the order of the configuration from highest to lowest value of average magnetic flux density are as follows: 4 mm (0.205 T), 3 mm (0.185

T), 2 mm (0.145 T), and 1 mm (0.093 T). Based on this order, the thickness of 4 mm yields the highest value of magnetic flux density among the other three. Therefore, it can be concluded that, the thicker the plates, the better the distribution of flux density due to the larger surface area. Thus, the 4 mm is selected for the design of MRE bushing.

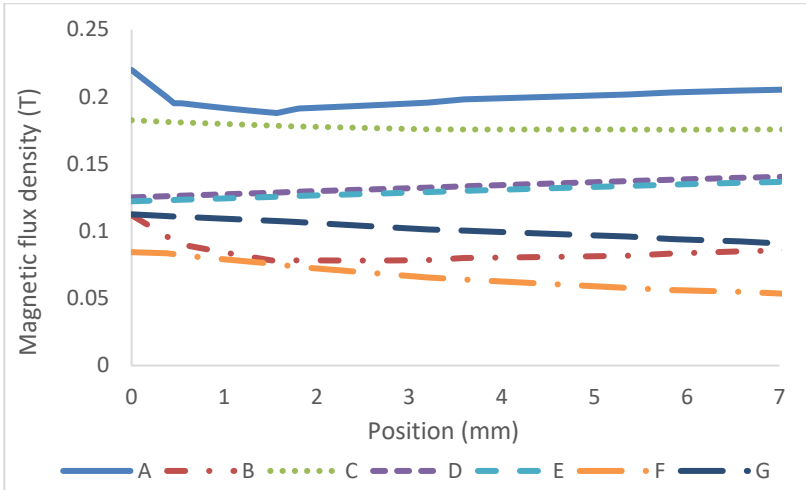

Figure 7: Magnetic flux density for different configurations of materials

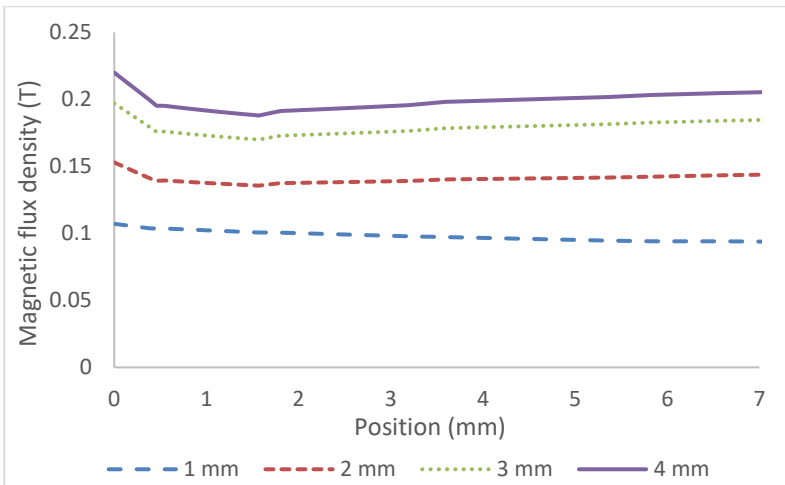

Figure 8: Magnetic flux density for difference thickness

Dynamic stiffness

After the frequency sweep experiment on the MRE bushing, the result of dynamic stiffness is obtained as shown in Figure 9. As can be seen from the graph, the stiffness is increased by increasing the frequency from 1 to 15 Hz and the input current from 0.5 to 2.5 A. Table 5 shows the result of dynamic stiffness at different current input and frequencies.

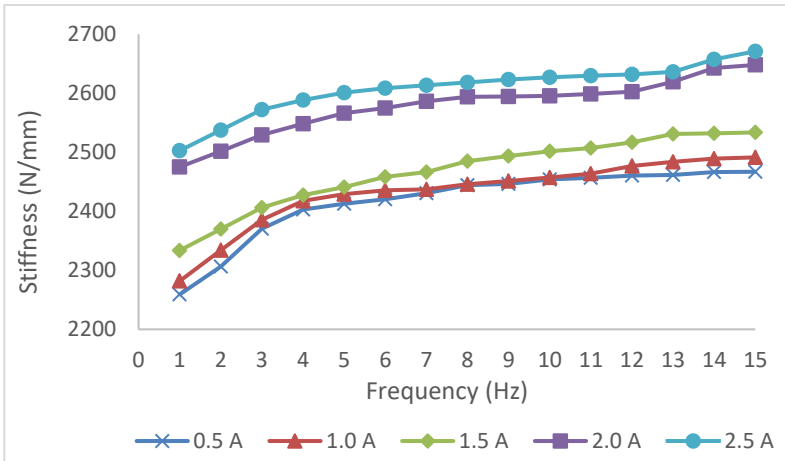

Figure 9: Stiffness of MRE bushing with varies applied current

Table 5: Result of dynamic stiffness at different current input and frequencies

Current	Frequency	
	1 Hz	15 Hz
0.5 A	2259.13 N/mm	2466.98 N/mm
1.0 A	2281.87 N/mm	2491.38 N/mm
1.5 A	2333.75 N/mm	2533.62 N/mm
2.0 A	2475.15 N/mm	2648.01 N/mm
2.5 A	2502.74 N/mm	2671.06 N/mm

Accordingly, the stiffness has been steadily increased when the applied current is from 0.5 to 2.5 A. The percentage increment for the stiffness from minimum applied current (0.5 A) to maximum applied current (2.5 A) for low frequency (1 Hz) and high frequency (15 Hz) are 10.78% and 7.52% respectively. Due to the stiffness of MRE being dependent on the magnetic field, the applied current plays the main role to change the stiffness. As the magnetic field strength increases, the stiffness of MRE can be significantly increased [29]. The results revealed that the MRE bushing is stiffer when more input currents and frequencies are applied. This is because when more input

current is applied, the magnetic field strength is increasing in the bushing which causes the bushing to become stiffer. On the other hand, as the frequencies increased, the stiffness of the bushing increased as well as is related to a high amount of vibration applied to the bushing. It is a regular occurrence in viscoelastic materials that frequency intensities will lead to increased intricacy in the matrix since the deformation of molecule chains has failed to keep up with the shear force, hence causing the stiffness to increase with increasing frequency intensities [30]. Thus, the bushing tends to act stiffer for vibration absorption. This is beneficial for the suspension system as stiff suspension bushing yields excellent handling, while softer suspension bushing improved ride comfort significantly [17].

Apart from that, dramatic changes in the stiffness behavior can be seen between the applied current of 1.5 A and 2.0 A for all excitation frequencies. The applied current in this study can be classified into two categories which are as low current range (0.5-1.5 A) and the high current range (2.0-2.5 A). When the high current is applied, it leads to a high magnetic flux density in the MRE bushing which attributed to the MRE compound rigidity and increasing the stiffness abilities. Here, the carbonyl iron particles (CIPs) are well-embedded and randomly distributed in the matrix. CIPs are a soft magnetic material which has an obvious active response to the presence of the magnetic field. The application of high current triggered the magnetic particles to react rigorously towards the compound. This phenomenon is related to the magnetic saturation and coercivity force [31]. As the magnetic field intensity keep increasing, it reduced the displacement between the particles as a result of strong interaction that had linked the particles in the matrix. The reduced distance between the magnetic particles leads to a stronger bonding interaction of magnetic particles in the MRE bushing. The magnetic field will continuously trigger the magnetic particles until achieving saturation point. Therefore, that is the reason for the significant changes in stiffness between low and high applied currents. The stiffness, in this case, strongly depended on the strength of the magnetic field.

Therefore, this MRE bushing is able to achieve variable stiffness behavior. All in all, it can be observed that the stiffness of MRE bushing is increasing according to the intensity of the magnetic field.

Conclusions

In this paper, an MRE bushing is simulated to study the effects of various configurations such as coil, materials, and geometrical dimensions of the part used in the bushing. The conceptual design of MRE bushing undergoes the analysis of magnetic flux density by FEMM simulation, where the magnetic flux density across the MRE effective area has been maximised based on different configurations applied. It can be noted that the use of a single coil,

the use of magnetic material for all parts except the coil bobbin, and the higher thickness of the ring plates can help to maximise the magnetic field strength in the bushing. The best configuration based on simulation analysis is achieved and that design proceeds for the experimental testing of dynamic stiffness. Based on the experimental test, the variable stiffness behavior of MRE bushing can be determined, where the higher magnetic field strength provides higher stiffness significantly. It is found that the changes in current and frequencies caused changes in the dynamic stiffness of the bushing. Thus, it has proven the concept of MRE as a smart material, which should be explored more and intensely reinvestigated in the future. In a nutshell, MRE bushing is potential as a vibration control in automotive applications especially in suspension systems due to its behaviour which is adjustable, tuneable, and controllable stiffness.

Contributions of Authors

M.I.A.H.: writing—original draft preparation, methodology, investigation, validation; A.Y.A.F., N.A.N. and S.A.M.: supervision, conceptualization, writing—reviewing and editing, funding acquisition; U.U., F.I. and I.I.: writing—review and editing. All authors have read and agreed to the published version of the manuscript.

Funding

This research work is supported and funded by Universiti Teknologi Malaysia (UTM) under UTM Prototype Research Grant (UTMPR) (Vot no. 00L46). The authors also thank Japan International Cooperation Agency Fund (JICA Fund) (Vot no. 4B696).

Conflict of Interests

The authors declare no conflict of interest. The authors also declare that they have no known competing financial interests or personal relationships that could have appeared to influence the work reported in this paper.

Acknowledgement

Million thanks to the Engineering Materials and Structures group member (eMast iKohza), Universiti Teknologi Malaysia that always provide morale support and constructive discussion throughout the research work.

References

[1] M.A. Faizal Johari, S.A. Mazlan, Ubaidillah, et al, "An Overview of Durability Evaluations of Elastomer-Based Magnetorheological Materials," *IEEE Access, vol.* 8, pp. 134536–134552, 2020.

[2] S.A.B.A. Aziz, S.A. Mazlan, N.A. Nordin, et al., "Material characterization of magnetorheological elastomers with corroded carbonyl iron particles: Morphological images and field-dependent viscoelastic properties," *International Journal of Molecular Sciences*; vol. 20, pp. 1-20, 2019.

[3] G. Zhang, Zhang J, Guo X, et al., "Effects of graphene oxide on microstructure and mechanical properties of isotropic polydimethylsiloxane-based magnetorheological elastomers," *Rheologica Acta*, vol. 61, pp. 215–228, 2022.

[4] S. Eraslan, I.M. Gitman, H. Askes, et al., "Determination of representative volume element size for a magnetorheological elastomer," *Computational Materials Science*; vol. 203, pp. 11070, 2022.

[5] Yunus NA, Mazlan SA, Ubaidillah, et al., "Rheological properties of isotropic magnetorheological elastomers featuring an epoxidized natural rubber," *Smart Materials and Structures*, vol. 25, pp. 1–11, 2016.

[6] Shabdin MK, Zainudin AA, Mazlan SA, et al., "Tunable low range Gr induced magnetorheological elastomer with magnetically conductive feedback" *Smart Materials and Structures*, vol. 29, no. 5, 2020.

[7] Zainudin AA, Yunus NA, Mazlan SA, et al., "Rheological and resistance properties of magnetorheological elastomer with cobalt for sensor application",. *Applied Sci*ences, vol. 10, no. 5, pp. 1638, 2020.

[8] Burhannuddin NL, Nordin NA, Mazlan SA, et al., "Physicochemical characterization and rheological properties of magnetic elastomers containing different shapes of corroded carbonyl iron particles," *Scientific Reports*, vol. 11, pp 1–17, 2021.

[9] Khairi MHA, Fatah AYA, Mazlan SA, et al., "Enhancement of particle alignment using silicone oil plasticizer and its effects on the field-dependent properties of magnetorheological elastomers," *International Journal of Molecular Sciences*, vol. 20, no. 17, 2019.

[10] Gong XL, Zhang XZ, Zhang PQ, "Fabrication and characterization of isotropic magnetorheological elastomers," *Polymer Testing, vol. 24, no. 5, pp. 669-676,* 2005.

[11] Liu T, Xu Y., "Magnetorheological Elastomers: Materials and Applications," Smart and Functional Soft Materials, 2019.
[12] Ubaidillah, Sutrisno J, Purwanto A, et al., "Recent progress on magnetorheological solids: Materials, fabrication, testing, and applications," *Advanced Engineering Materials,* vol. 17, no. 5, pp. 563-597, 2015.
[13] Wahab NAA, Mazlan SA, Ubaidillah, et al., "Fabrication and investigation on field-dependent properties of natural rubber based magneto-rheological elastomer isolator," *Smart Materials and Structures,* vol. 5, no. 11, pp. 1-11, 2016.
[14] Kang SS, Choi K, Nam J Do, et al. Magnetorheological elastomers: Fabrication, characteristics, and applications. *Materials* 2020; 13: 1–24.
[15] Jang DI, Yun GE, Park JE, et al., "Designing an attachable and power-efficient all-in-one module of a tunable vibration absorber based on magnetorheological elastomer" *Smart Materials and Structures*, vol. 27, 2018.
[16] Ubaidillah, Hadi S, Harjana, et al., "Design and fabrication of magnetorheological elastomer vibration isolator," *Journal of Mechanical Engineering*, vol. 5, no. 6, pp. 192-210, 2018.
[17] Kumbhar SR, Maji S, Kumar B., "Development and Testing of MRE Bushing for Road Vehicle Suspension System," *International Journal of Recent Advances in Mechanical Engineering*, vol. 2, no. 3, 2013.
[18] Abdelfatah MM. *Magnetorheological bushing steering system*. US, 2018.
[19] Elie LD, Ginder JM, Stewart WM, et al. *Variable Stiffness Bushing using Magnetorheological Elastomer*. European, 2002.
[20] Ginder JM, Nichols ME, Elie LD, et al., "Controllable-Stiffness Components based on Magnetorheological Elastomers," *Smart Structures and Materials 2000: Smart Structures and Integrated Systems*. *SPIE*, vol. 3985, pp. 418, 2000.
[21] Ikeda K, Sakuragi A, of Japan B. *Rubber Bushing*. United State, 1993.
[22] Blom P, Kari L., "The frequency, amplitude and magnetic field dependent torsional stiffness of a magneto-sensitive rubber bushing," *International Journal of Mechanical Sciences*, vol. 60, no. 1, pp. 54-58, 2012.
[23] Kim SH, Park YJ, Cha AR, et al., "A feasibility work on the applications of MRE to automotive components," *IOP Conference Series: Materials Science and Engineering*, vol. 333, 2018.
[24] Lee HS, Shin JK, Msolli S, et al., "Prediction of the dynamic equivalent stiffness for a rubber bushing using the finite element method and empirical modeling," *International Journal of Mechanics and Materials in De*sign, vol. 15, no. 1, pp. 77–91, 2019.
[25] Ginder JM, Nichols ME, Elie LD, et al., "Magnetorheological Elastomers: Properties and Applications," *Smart Structures and Materials 1999. Smart Materials Technologies*, vol. 3675, pp. 131–138. 1999.

[26] Fatah AYA, Mazlan SA, Koga T, et al., “A review of design and modeling of magnetorheological valve,” *International Journal of Modern Physics B*, vol. 29, no. 4, 2015.

[27] Wahab NAA, Mazlan SA, Hairuddin K, et al., “Simulation study of electromagnetic circuit design in laminated magnetorheological elastomer isolator,” *IOP Conference Series Materials Science and Engineering*; vol. 100, no. 1, 2015.

[28] N.A. Wahab, S.A. Mazlan, F. Imaduddin, et al., "Development Of Magnetic Circuit Design In Multi Sandwich Magneto Rheological Elastomer (MRE) Isolator,” Journal of Physics Conference Series, vol. 1908, no. 1, pp. 2497-2508, 2016.

[29] A. Fuchs, Q. Zhang, J. Elkins, et al., "Development and characterization of magnetorheological elastomers," *Journal of Applied Polymer Science*, vol. 105, no. 5, pp. 2497–2508, 2007.

[30] Y.C. Fan, X.L. Gong, W.Q. Jiang, et al., "Effect of maleic anhydride on the damping property of magnetorheological elastomers," *Smart Materials and Structures*, vol. 19, no. 5, pp. 055015, 2010.

[31] N. Hapipi, S.A.A. Aziz, S.A. Mazlan, et al., "The field-dependent rheological properties of plate-like carbonyl iron particle-based magnetorheological elastomers," *Results in Physics*, vol. 12, pp. 2146–2154, 2019.